Letter

Power fluctuations in sheared amorphous materials: A minimal model

Timothy Ekeh,[1] Étienne Fodor,[2] Suzanne M. Fielding,[3] and Michael E. Cates[1]

[1]DAMTP, Centre for Mathematical Sciences, University of Cambridge, Wilberforce Road, Cambridge CB3 0WA, United Kingdom
[2]Department of Physics and Materials Science, University of Luxembourg, L-1511 Luxembourg, Luxembourg
[3]Department of Physics, Durham University, Science Laboratories, South Road, Durham DH1 3LE, United Kingdom

(Received 24 June 2021; accepted 9 February 2022; published 5 May 2022)

The importance of mesoscale fluctuations in flowing amorphous materials is widely accepted, without a clear understanding of their role. We propose a mean-field elastoplastic model that admits both stress and strain-rate fluctuations, and investigate the character of its power distribution under steady shear flow. The model predicts the suppression of negative power fluctuations near the liquid-solid transition; the existence of a fluctuation relation in limiting regimes but its replacement in general by stretched-exponential power-distribution tails; and a crossover between two distinct mechanisms for negative power fluctuations in the liquid and the yielding solid phases. We connect these predictions with recent results from particle-based, numerical microrheological experiments.

DOI: 10.1103/PhysRevE.105.L052601

Amorphous solids lack the translational order of crystals, but have more complicated viscoelastic responses than simple liquids. Examples include foams, gels, emulsions, granular materials, and glasses [1–3]. Although mechanically speaking these materials are solids at rest, they still have the ability to deform, and flow under a large enough external stress. Different flow behaviors can occur depending on the amplitude of the imposed stress or strain rate, and on internal properties of the system [4–6].

The *macroscopic* characterization of such flow regimes is well studied [1–3,7]. A more recent, contrasting theme is the important role of *fluctuations* [8,9] and avalanches [10,11] in large-scale flow. Advanced numerical simulations [12–14] have shown that rare dynamical events have significant impacts on mechanical behavior [15,16], contrary to common intuition. Importantly, the experimental sensitivity to measure temporal fluctuations of such flows has been achieved recently [10,17–21], offering a new testing ground for the ideas of stochastic thermodynamics [22]. These capabilities in numerical and laboratory experiments have delivered many novel observations, motivating detailed comparisons between these experiments and mesoscopic mean-field models. The latter provide idealized but nontrivial mechanistic accounts of the transition from fluid to yielding solid in terms of a few phenomenological parameters.

Despite their inevitable simplifications, such mean-field models have had remarkable successes [3,23,24]. However, none have fully addressed the rich phenomenology of fluctuations in dissipated power, including rare events in which the local stress and strain rates have opposite signs so that their product, the local power, becomes negative. Crucially, to capture these fluctuations both above and below jamming, the stress and the strain rate must both be able to fluctuate [25].

Among mesoscopic models, those based on elastoplastic concepts have a long history [3,13,26–33], and some are equipped to deal with rheological fluctuations, particularly the Hebraud-Lequeux (HL) model, which treats the local stress as a stochastic process subject to constant shear and mechanical noise [23] (Fig. 1). The noise captures at the mean-field level (without spatial information) avalanches of stress elsewhere in the system [30,34]. The soft glassy rheology (SGR) approach also assumes a uniform strain rate, with a locally stochastic stress proportional to elastic deformation [24]. Thus HL and SGR both lack the key feature of independent fluctuations in local shear rate *and* local stress.

Such fluctuations are restored in models of elastoplastic elements coupled by explicit dynamical rules, in two or more dimensions [11,35–39]. However, while these models usefully bridge between first-principles studies and mean-field models such as HL and SGR, they generally defy analytic progress, limiting their explanatory power.

In this Letter, we propose a minimal, mean-field elastoplastic model, in which HL-type stress elements are grouped into M sets of members $k \in \{1, \dots, N\}$ with a common strain rate $\dot{\gamma}$. Below, we use our model to study fluctuations in the *local power*, an interesting observable in flowing amorphous materials, focusing particularly on negative power fluctuations. Importantly, we show that the model captures an intriguing crossover in the dominant mechanism for such fluctuations whereby they are carried primarily by local reversals *in stress* when the system is well below its jamming transition, but in *strain rate* when well above it [25]. Besides this, we find that the power distribution has power-law tails, and discuss the extent to which it exhibits fluctuation relations analogous to those seen in thermal driven systems [22,40–43]. Overall, our minimal model offers a tractable framework to rationalize the generic character of power fluctuations in a broad class of sheared amorphous materials.

We shall refer to our minimal model as the N-element HL model, or NHL. A geometrical interpretation (Fig. 1) is to suppose that $\dot{\gamma}$ varies in the velocity-gradient direction only, and then impose by force balance the same macroscopic stress

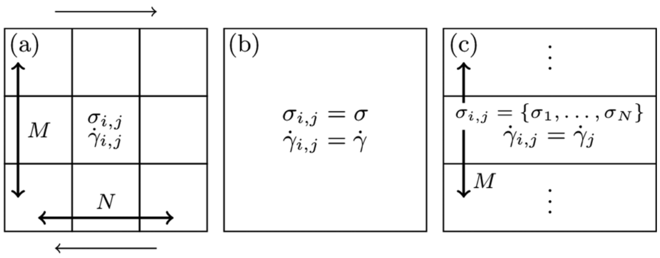

FIG. 1. (a) Fully resolved, lattice-based $M \times N$ system of elemental stresses $\sigma_{i,j}$ and strain rates $\dot\gamma_{i,j}$, with external shear applied at boundaries. (b) The zero-dimensional HL model discards any notion of space at the mean-field level [23]. (c) Our extended model homogenizes strain rate $\dot\gamma$ along, but allows stochastic variation between, streamlines [44]. Each streamline $j \in \{1, \ldots, M\}$ carries a set of N stress elements σ_k with no further spatial structure, creating an effectively 1D model with translational symmetry along the flow direction.

on all the M streamlines, each carrying N fluctuating stress elements, without further spatial structure. This geometrical construction of NHL follows that for the SGR-based model developed in Ref. [44] to discuss aging in shear bands. Standard HL is recovered as $N \to \infty$, whereas finite N might reflect a finite *coherence length* along streamlines, beyond which elements no longer share a common strain rate.

HL model [23]. In the HL model, the probability distribution $f(\sigma, t)$ for elemental stresses evolves as

$$\partial_t f = -\dot\gamma \partial_\sigma f + D(t)\partial_\sigma^2 f - r(\sigma) f + \frac{D(t)}{\alpha}\delta(\sigma), \quad (1)$$

$$D(t) = \alpha \int r(\sigma') f(\sigma', t) d\sigma'. \quad (2)$$

Here, each element is statistically identical, so no spatial index arises. The terms on the right-hand side in (1) originate as follows. The first is the advective distortion of stress elements at shear rate $\dot\gamma$: The material responds elastically (with modulus unity) in the absence of plastic events. The second term encodes the local presence of mechanical noise, resulting from plastic events elsewhere, in an effective diffusivity D [31]. The final two terms describe a resetting mechanism, which causes stress elements to relax to a completely unstressed state. For simplicity, its rate is chosen as $r(\sigma) = H(|\sigma| - \sigma_c)/\tau$, with H the Heaviside function, so that resetting occurs only when $|\sigma|$ exceeds a threshold σ_c. The global rate of these jumps then sets the noise level D via (2). In what follows, we choose units such that $\tau = \sigma_c = 1$.

HL captures the transition from liquid to yielding solid on varying the parameter α: At small $\dot\gamma$ the average stress $\langle\sigma\rangle$ scales as $\dot\gamma$ for $\alpha > \alpha_c = 1/2$ (the liquid phase) but converges to a yield stress σ_y for $\alpha < \alpha_c$ (the solid).

Note that the diffusivity D does not vanish at $\dot\gamma \to 0$ in the liquid phase. This feature is counterintuitive, as noted in Ref. [26], since D is related to the rate of stress resetting events, which should not occur in the absence of shearing. The HL liquid thus requires energy input, e.g., from the aging of unresolved degrees of freedom. However, this quasithermal process does not interfere with the stress and strain energetics considered here.

Setup of NHL model. In contrast with standard HL, we now promote the shear rate $\dot\gamma$ to a fluctuating quantity alongside the stochastic stress variable σ. To achieve this, we can impose a spatial force balance in the direction(s) perpendicular to the shear. Consider in $d = 2$ a subvolume of $M \times N$ elastoplastic sites, each endowed with a coarse-grained stress $\sigma_{i,j}$ and local shear rate $\dot\gamma_{i,j}$, where i, j are spatial indices. Here, the shear rate is the local value seen by an element, which is not uniform in general. For simplicity, however, we assume it remains uniform along streamlines, whose direction is set by boundary shearing, so that $\dot\gamma_{i,j} = \dot\gamma_j$ for all i.

This assumption effectively segments the subvolume into M separate streamlines, each containing N elements (see Fig. 1). Moreover, because in HL the flow curve (steady-state macroscopic stress versus strain rate) is monotonic —a feature shared by NHL as we show in the Supplemental Material [45]—we can exclude macroscopic inhomogeneities such as shear banding in the steady state [46]. All streamlines then have identical statistics for the fluctuating shear rate ($\dot\gamma_j = \dot\gamma$) as well as for the N elemental stresses $\{\sigma_1 \ldots \sigma_k, \ldots \sigma_N\}$; the value of M (as the index j) plays no further role. The dynamics for each elemental stress σ_k on any chosen streamline should obey (1) and (2) but with advection now controlled by the instantaneous *local* shear rate $\dot\gamma(t)$.

Neglecting inertia, we now add a Newtonian background fluid of viscosity η. Force balance then requires that the total shear stress Σ is independent of streamline:

$$\Sigma = \frac{1}{N}\sum_{k=1}^{N} \sigma_k + \eta\dot\gamma. \quad (3)$$

This use of force balance [44] is standard, e.g., Ref. [46]. Equation (3) means the local shear rate adapts instantaneously to the random realizations of the stresses σ_k in N elements, each equipped with its own mechanical noise. Clearly, therefore, $\dot\gamma$ is now a stochastic variable. Indeed, between successive resettings, the stresses σ_k and shear rate $\dot\gamma$ follow coupled stochastic equations [45],

$$d\sigma_k = \dot\gamma dt + \sqrt{2D} dW_k, \quad \eta d\dot\gamma = -\dot\gamma dt - \frac{\sqrt{2D}}{N}\sum_{k=1}^{N} dW_k,$$

with dt the time step, and dW_k a set of N independent, unit-variance Wiener processes: $dW_i dW_j = \delta_{ij} dt$ [47]. The diffusivity D is set by the total jump rate within our set of N elements, coupling these together. In stochastic simulations we evaluate $D = \tilde D \equiv \alpha \sum_k r(\sigma_k)/N$ directly, whereas our mean-field analyses use (2). Note that alternatively one might evaluate D as $D = \langle \tilde D \rangle_M$ averaged across M stochastic samples from the same distribution, representing different streamlines. This choice reintroduces M as a parameter, couples otherwise independent streamlines, and increases sampling costs M-fold; we parsimoniously reject it.

The joint distribution $P(\sigma, \dot\gamma, t)$ can be obtained explicitly, although its form is unwieldy. To simplify matters, we now take P to be separable. This assumption is exact as $N \to \infty$ and also captures the physics at large finite N [45], as we confirm by direct stochastic simulations be-

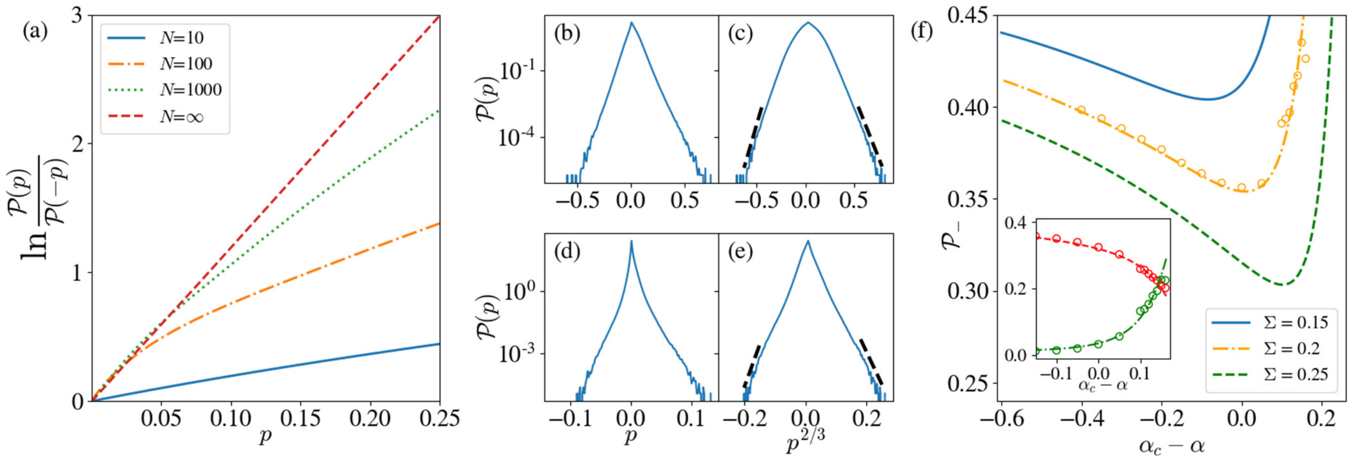

FIG. 2. (a) The log ratio of the power distribution is plotted for HL ($N \to \infty$), and for NHL at various finite N. The straight line for HL follows from the fluctuation relation (7), which breaks down at finite N. Common parameters for the lines at finite N are $\alpha = 0.8$, $\Sigma = 0.2$, and $\eta = 0.1$. The $N = \infty$ curve is produced with $\alpha = 0.8$, and $\dot{\gamma} = 0.07$, which is the common mean shear rate for the NHL models. (b)–(e) Power distribution on either side of the yielding transition. In the fluid regime [(b), (c) $\alpha = 0.70$], the decays could be mistaken for a two-sided exponential. In the yielding solid regime [(d), (e) $\alpha = 0.37$], there is a clear departure from the two-sided exponential. The right panels are fit-free plots of $\mathcal{P}$ against $p^{2/3}$ to test (8) which predicts linear behavior as a function of $p^{2/3}$. The remaining parameters are $\eta = 0.1$, $\Sigma = 0.2$, $N = 2^{10}$. (f) The probability $\mathcal{P}(p < 0)$ of negative injected power is nonmonotonic in α. The inset decomposes this into $(\sigma^+, \dot{\gamma}^-)$ (green dots and dashes) and $(\sigma^-, \dot{\gamma}^+)$ (red dashed line) for $\Sigma = 0.2$, showing the crossover on moving from afluid to solid phase. Same parameters as in (b)–(e). Lines are from numerical solutions of (4) and (5) and circles are stochastic simulations of the full NHL dynamics. As N increases, the minimum deepens and moves to the right, and it vanishes for $N \to \infty$.

low. The marginal distributions $f(\sigma, t) = \int P(\sigma, \dot{\gamma}, t) d\dot{\gamma}$ and $g(\dot{\gamma}, t) = \int P(\sigma, \dot{\gamma}, t) d\sigma$ then evolve as

$$\partial_t f = -\langle\dot{\gamma}\rangle \partial_\sigma f + D(t)\partial_\sigma^2 f - r(\sigma) f + \frac{D(t)}{\alpha}\delta(\sigma), \quad (4)$$

$$\partial_t g = \partial_{\dot{\gamma}}\left[\frac{\dot{\gamma} - \langle\sigma r(\sigma)\rangle}{\eta} g\right] + \partial_{\dot{\gamma}}^2\left[\frac{2D(t) + \langle\sigma^2 r(\sigma)\rangle}{2\eta^2 N} g\right], \quad (5)$$

where averages $\langle\cdot\rangle$ are taken over $P(\sigma, \dot{\gamma}, t)$. The equation for f is exactly that of the HL model (1) under the action of the average shear $\langle\dot{\gamma}\rangle$; the local shear rate $\dot{\gamma}$ is a mean-reverting process, whose fluctuations depend on the dynamics of the N elements.

Standard HL is recovered in the limit $N \to \infty$, when all elements in a bulk system share a common shear rate $\dot{\gamma}$. In that limit, force balance gives $\dot{\gamma} = (\Sigma - \langle\sigma\rangle)/\eta$, since the average of N stresses in (3) converges to the ensemble average $\langle\sigma\rangle$. Accordingly the shear rate does not fluctuate, although the elemental stress values still do so, sampling the HL steady-state stress distribution $f(\sigma)$ whose support (for $\dot{\gamma} > 0$) includes negative σ values.

For finite N, fluctuations in $\dot{\gamma}$ allow a much richer picture as explored below. Nonetheless, many macroscopic features of standard HL remain intact. Specifically, the fluid-solid transition still occurs at $\alpha_c = 1/2$ and, because the NHL stress equation (4) recovers HL on setting $\langle\dot{\gamma}\rangle \to \dot{\gamma}$, the macroscopic stress $\sigma_M = \langle\sigma\rangle$ behaves the same way. Thus NHL's flow curves $\sigma_M(\dot{\gamma})$, as those of HL, show Newtonian, power-law fluid, and Herschel-Bulkley behaviors for $\alpha > \alpha_c$, $\alpha = \alpha_c$, and $\alpha < \alpha_c$, respectively [23]. One difference is that in NHL the formal control parameter is Σ rather than $\langle\dot{\gamma}\rangle$ as usually chosen in HL. However, for a bulk system under uniform flow, these two quantities are related by the flow curve, and the two ensembles should give similar distributions for fluctuating element stresses. Note that this breaks down when considering coupling between streamlines.

Power distribution. We consider the distribution $\mathcal{P}(p, t)$ of power injected into elements, $p = \sigma\dot{\gamma}$ (Fig. 2):

$$\mathcal{P}(p, t) = \int \delta(p - \dot{\gamma}\sigma) P(\sigma, \dot{\gamma}, t) d\sigma d\dot{\gamma}. \quad (6)$$

Power injected directly into the background fluid, $\eta\dot{\gamma}^2$, is excluded. In the HL limit ($N \to \infty$), the steady-state distribution reduces to $\mathcal{P}(p) = (1/\dot{\gamma}) f_{\mathrm{HL}}(p/\dot{\gamma})$, where f_{HL} is the stress distribution of (1), with known form [23,26,45]. This gives rise to the *fluctuation relation* (FR)

$$\ln \frac{\mathcal{P}(p)}{\mathcal{P}(-p)} = \frac{p}{D}, \quad (7)$$

where D is the steady-state diffusivity from (2). The FR indicates that negative power fluctuations, where stress and strain rate have locally opposite signs, are exponentially rarer than their positive counterparts, $\mathcal{P}(-p) = \mathcal{P}(p) e^{-p/D}$, and they vanish altogether as $D \to 0$. For HL, this relation is a direct consequence of the distribution's tails decaying exponentially [45]. For thermal stochastic processes, FRs resembling (7) hold in a broader context, without relying on any specific form of distribution, and they have been linked to microscopic reversibility [22,40–43]. Such relations have also been reported in other nonequilibrium contexts [48–53], in some cases defining an effective temperature [54].

Numerical evidence for the linear p dependence in (7) was presented in Ref. [25]. However, an analysis of (4) and (5) suggests this result is far from universal for rheological fluctuations in amorphous materials. First, we find that even in the HL limit, $N \to \infty$, (7) breaks down if one chooses a resetting rule asymmetric in σ, such as $r(\sigma) = H(|\sigma - \sigma_0| - 1)$ [55], as might encode the structural memory of past flow [56]. Second, even with symmetric resetting, the FR (7) is not only inexact for $N < \infty$, but quite inaccurate for $N \lesssim 1000$. This is clear from $\ln[\mathcal{P}(p)/\mathcal{P}(-p)]$ as calculated from (4) and (5) and plotted in Fig. 2(a). Strikingly, for our NHL model, the decays of the distribution are no longer exponential: Figs. 2(b)–2(e) show the full $\mathcal{P}(p)$ found by stochastic simulation. Moreover, from (4) and (5) we obtain the cumulative function $\mathcal{P}(p > p_l) = \int_{p_l}^{\infty} \mathcal{P}(p)dp$ for large p_l [45], which reveals stretched-exponential tails,

$$\log \mathcal{P}(\pm p) \underset{|p|\to\infty}{\sim} -c_{\pm}|p|^{2/3}, \tag{8}$$

with $c_{\pm}$ parameter-dependent constants for positive and negative power [45]. These vanish as $N \to \infty$ recovering the HL result; for finite N, we show in the Supplemental Material [45] that the asymptotes obeying (8) emerge for $|p| \gg \sqrt{\mathrm{Var}(\dot{\gamma})}$, where $\mathrm{Var}(\dot{\gamma})$ decreases with N.

Mechanisms for negative power. To get further insight from our minimal NHL model, we consider the probability to observe negative power, $\mathcal{P}_- = \int_{-\infty}^{0} \mathcal{P}(p)dp$. This follows from (6) as

$$\mathcal{P}_- = \frac{1}{2} - \frac{1}{2}\mathrm{erf}\left(\frac{\langle\dot{\gamma}\rangle}{\sqrt{2\mathrm{Var}(\dot{\gamma})}}\right) \int f(\sigma)\frac{|\sigma|}{\sigma}d\sigma, \tag{9}$$

where $\mathrm{erf}(z) = \frac{2}{\sqrt{\pi}}\int_0^z e^{-t^2}dt$ is the usual error function. We predict analytically, and confirm by stochastic simulations, a nonmonotonic behavior of $\mathcal{P}_-$ on varying the distance from the fluid-solid transition point $\alpha_c - \alpha$ [see Fig. 2(f)]. Negative power fluctuations are enhanced deep in both the fluid ($\alpha_c \gg \alpha$) and yielding solid ($\alpha_c \ll \alpha$). Although the minimum lies close to the transition point for the case shown, this positioning is *not universal* but depends on a nontrivial combination of model parameters, crucially including N, with the consequence that the upturn of $\mathcal{P}_-(\alpha)$ in the yielding solid phase moves to ever larger $\alpha_c - \alpha$ as $N \to \infty$. Our finding of a minimum in NHL is consistent with the first-principles simulations of Ref. [25], but our calculations do not support any claim that this lies universally at $\alpha = \alpha_c$. Another difference is that generically our minimum is shallow whereas Ref. [25] reports $\mathcal{P}_-$ close to zero there.

Further insight can be gained by noting that a negative realization of the local power $p = \sigma\dot{\gamma}$ is achieved when either $\sigma > 0$ and $\dot{\gamma} < 0$ $(\sigma^+, \dot{\gamma}^-)$, or $\sigma < 0$ and $\dot{\gamma} > 0$ $(\sigma^-, \dot{\gamma}^+)$. Since these classes are mutually exclusive, one can consider them as separate mechanisms contributing to the negative power probability $\mathcal{P}_-$. The inset in Fig. 2(f) shows how $\mathcal{P}_-$ decomposes into these contributions. Crucially, we observe a crossover from the $(\sigma^-, \dot{\gamma}^+)$ channel in the fluid phase to the $(\sigma^+, \dot{\gamma}^-)$ channel in the yielding solid. This agrees with Ref. [25], where these channels are respectively linked to collisions of deformable particles across and along the compression direction. Within NHL, this crossover is a physically natural consequence of variations in the width of the shear rate distribution $g(\dot{\gamma})$. Deep in the fluid regime, the ratio of the mean shear rate $\langle\dot{\gamma}\rangle$ to its standard deviation $\sqrt{\mathrm{Var}(\dot{\gamma})}$ is large, so that g is peaked at $\dot{\gamma} = \langle\dot{\gamma}\rangle > 0$ with little weight at $\dot{\gamma} < 0$. In contrast, deep in the yielding regime, this ratio is much smaller, so that instantaneous reversals of the shear rate are much more likely.

Discussion. It is remarkable that the features of $\mathcal{P}_-(\alpha)$ mentioned above, including its decomposition into two distinct mechanisms, are explicable in outline within a mean-field approach, with no appeal to fully nonlinear many-body fluctuations or critical phenomena [57], even if these may also be present. Success of the mean-field model depends on allowing fluctuations in the shear rate as well as stress; this is achieved in NHL, but suppressed in the HL limit ($N \to \infty$). Strikingly, these same shear rate fluctuations are directly responsible for violations of the FR (7). Accordingly, we expect such violations to be most easily detectable in the yielding solid phase, rather than in relatively dilute fluid systems or other conditions with a negligible shear rate variation.

Concluding remarks. In this Letter, we proposed an elastoplastic model, called NHL, of microrheological fluctuations, focusing on power fluctuations. It represents a minimal extension of the Hebraud-Lequeux (HL) model [23], allowing stress and strain rate to fluctuate on similar terms. An open question is the origin of the parameter N. We said this could relate to a streamwise coherence length for the flow, but NHL itself contains no such spatial information: The number N of stress elements that share a common $\dot{\gamma}$ is undetermined. However, the more relevant physical observable is Nn, with n the number of primary particles defining a stress element. This n is similarly undetermined in mesoscopic models [23,24,31,56]. Plausibly, N could depend on macroscopic flow conditions, or proximity to the jamming transition, but not on the power p in a given local fluctuation. Accordingly our main predictions for the power distribution $\mathcal{P}(p)$ should be robust. These predictions comprise a generic violation of the FR (7), stretched-exponential tails (8), and a minimum in $\mathcal{P}(p < 0)$ near the fluid-solid transition, caused by a crossover between fluctuations with negative local stress and negative local shear rate [Fig. 2(f)].

As possible extensions of our work, one could build analogous models using other elastoplastic frameworks, such as SGR [24], investigate the effects of noise distributions with fat tails [28,34], or address the coupling between streamlines to explore how instabilities such as shear banding [46] influence power fluctuation statistics. It would be interesting to investigate other amorphous systems in a similar way. Previous numerical studies have looked at the detailed statistics of other fluctuating observables with both molecular dynamics simulations and spatial elastoplastic models [11,15,34,38]. Therefore adapting to the study of the injected power observable instead is likely to be straightforward. Furthermore, experimental setups now exist which can measure local stress tensor fluctuations at millisecond resolution [10].

Acknowledgments. This work has received funding from the European Research Council (ERC) under the EU's Horizon 2020 Programme, Grant Agreements No. 740269 and No. 885146. This research was funded in part by the Luxembourg National Research Fund (FNR), Grant Reference No. 14389168. M.E.C. is funded by the Royal Society.

[1] L. Berthier and G. Biroli, Theoretical perspective on the glass transition and amorphous materials, Rev. Mod. Phys. **83**, 587 (2011).
[2] D. Bonn, M. M. Denn, L. Berthier, T. Divoux, and S. Manneville, Yield stress materials in soft condensed matter, Rev. Mod. Phys. **89**, 035005 (2017).
[3] A. Nicolas, E. E. Ferrero, K. Martens, and J.-L. Barrat, Deformation and flow of amorphous solids: Insights from elastoplastic models, Rev. Mod. Phys. **90**, 045006 (2018).
[4] J. D. Martin and Y. T. Hu, Transient and steady-state shear banding in aging soft glassy materials, Soft Matter **8**, 6940 (2012).
[5] P. Coussot, Q. D. Nguyen, H. T. Huynh, and D. Bonn, Avalanche Behavior in Yield Stress Fluids, Phys. Rev. Lett. **88**, 175501 (2002).
[6] J. Paredes, N. Shahidzadeh-Bonn, and D. Bonn, Shear banding in thixotropic and normal emulsions, J. Phys.: Condens. Matter **23**, 284116 (2011).
[7] J. S. Langer, Shear-transformation-zone theory of yielding in athermal amorphous materials, Phys. Rev. E **92**, 012318 (2015).
[8] D. Lootens, H. Van Damme, and P. Hébraud, Giant Stress Fluctuations at the Jamming Transition, Phys. Rev. Lett. **90**, 178301 (2003).
[9] P. Jop, V. Mansard, P. Chaudhuri, L. Bocquet, and A. Colin, Microscale Rheology of a Soft Glassy Material Close to Yielding, Phys. Rev. Lett. **108**, 148301 (2012).
[10] A. L. Thomas, Z. Tang, K. E. Daniels, and N. M. Vriend, Force fluctuations at the transition from quasi-static to inertial granular flow, Soft Matter **15**, 8532 (2019).
[11] C. Liu, E. E. Ferrero, F. Puosi, J.-L. Barrat, and K. Martens, Driving Rate Dependence of Avalanche Statistics and Shapes at the Yielding Transition, Phys. Rev. Lett. **116**, 065501 (2016).
[12] A. Ninarello, L. Berthier, and D. Coslovich, Models and Algorithms for the Next Generation of Glass Transition Studies, Phys. Rev. X **7**, 021039 (2017).
[13] M. Ozawa, L. Berthier, G. Biroli, A. Rosso, and G. Tarjus, Random critical point separates brittle and ductile yielding transitions in amorphous materials, Proc. Natl. Acad. Sci. USA **115**, 6656 (2018).
[14] L. Berthier, E. Flenner, C. J. Fullerton, C. Scalliet, and M. Singh, Efficient swap algorithms for molecular dynamics simulations of equilibrium supercooled liquids, J. Stat. Mech. **(2019)**, 064004.
[15] M. Ozawa, L. Berthier, G. Biroli, and G. Tarjus, Role of fluctuations in the yielding transition of two-dimensional glasses, Phys. Rev. Research **2**, 023203 (2020).
[16] M. Ozawa, L. Berthier, G. Biroli, and G. Tarjus, Rare events and disorder control the brittle yielding of amorphous solids, arXiv:2102.05846.
[17] B. Miller, C. O'Hern, and R. P. Behringer, Stress Fluctuations for Continuously Sheared Granular Materials, Phys. Rev. Lett. **77**, 3110 (1996).
[18] E. D. Knowlton, D. J. Pine, and L. Cipelletti, A microscopic view of the yielding transition in concentrated emulsions, Soft Matter **10**, 6931 (2014).
[19] K. W. Desmond and E. R. Weeks, Measurement of Stress Redistribution in Flowing Emulsions, Phys. Rev. Lett. **115**, 098302 (2015).
[20] V. Chikkadi, G. Wegdam, D. Bonn, B. Nienhuis, and P. Schall, Long-Range Strain Correlations in Sheared Colloidal Glasses, Phys. Rev. Lett. **107**, 198303 (2011).
[21] J. Zheng, A. Sun, Y. Wang, and J. Zhang, Energy Fluctuations in Slowly Sheared Granular Materials, Phys. Rev. Lett. **121**, 248001 (2018).
[22] U. Seifert, Stochastic thermodynamics, fluctuation theorems and molecular machines, Rep. Prog. Phys. **75**, 126001 (2012).
[23] P. Hébraud and F. Lequeux, Mode-Coupling Theory for the Pasty Rheology of Soft Glassy Materials, Phys. Rev. Lett. **81**, 2934 (1998).
[24] P. Sollich, F. Lequeux, P. Hébraud, and M. E. Cates, Rheology of Soft Glassy Materials, Phys. Rev. Lett. **78**, 2020 (1997).
[25] S. H. E. Rahbari, A. A. Saberi, H. Park, and J. Vollmer, Characterizing rare fluctuations in soft particulate flows, Nat. Commun. **8**, 11 (2017).
[26] E. Agoritsas, E. Bertin, K. Martens, and J.-L. Barrat, On the relevance of disorder in athermal amorphous materials under shear, Eur. Phys. J. E **38**, 71 (2015).
[27] L. Bocquet, A. Colin, and A. Ajdari, A Kinetic Theory of Plastic Flow in Soft Glassy Materials, Phys. Rev. Lett. **103**, 036001 (2009).
[28] J. T. Parley, S. M. Fielding, and P. Sollich, Aging in a mean field elastoplastic model of amorphous solids, Phys. Fluids **32**, 127104 (2020).
[29] M. Popović, T. W. J. de Geus, and M. Wyart, Elastoplastic description of sudden failure in athermal amorphous materials during quasistatic loading, Phys. Rev. E **98**, 040901(R) (2018).
[30] J. Lin, A. Saade, E. Lerner, A. Rosso, and M. Wyart, On the density of shear transformations in amorphous solids, Europhys. Lett. **105**, 26003 (2014).
[31] A. Nicolas, K. Martens, and J.-L. Barrat, Rheology of athermal amorphous solids: Revisiting simplified scenarios and the concept of mechanical noise temperature, Europhys. Lett. **107**, 44003 (2014).
[32] M. L. Goff, E. Bertin, and K. Martens, Giant fluctuations in the flow of fluidised soft glassy materials: An elasto-plastic modelling approach, J. Phys.: Mater. **3**, 025010 (2020).
[33] G. Picard, A. Ajdari, F. Lequeux, and L. Bocquet, Elastic consequences of a single plastic event: A step towards the microscopic modeling of the flow of yield stress fluids, Eur. Phys. J. E **15**, 371 (2004).
[34] J. Lin and M. Wyart, Mean-Field Description of Plastic Flow in Amorphous Solids, Phys. Rev. X **6**, 011005 (2016).
[35] A. Tanguy, F. Leonforte, and J.-L. Barrat, Plastic response of a 2D Lennard-Jones amorphous solid: Detailed analysis of the local rearrangements at very slow strain rate, Eur. Phys. J. E **20**, 355 (2006).
[36] M. L. Falk and J. S. Langer, Dynamics of viscoplastic deformation in amorphous solids, Phys. Rev. E **57**, 7192 (1998).
[37] C. E. Maloney and A. Lemaître, Amorphous systems in athermal, quasistatic shear, Phys. Rev. E **74**, 016118 (2006).
[38] A. Lemaître and C. Caroli, Plastic response of a two-dimensional amorphous solid to quasistatic shear: Transverse particle diffusion and phenomenology of dissipative events, Phys. Rev. E **76**, 036104 (2007).
[39] K. M. Salerno and M. O. Robbins, Effect of inertia on sheared disordered solids: Critical scaling of avalanches in two and three dimensions, Phys. Rev. E **88**, 062206 (2013).
[40] J. Kurchan, Fluctuation theorem for stochastic dynamics, J. Phys. A: Math. Gen. **31**, 3719 (1998).

[41] C. Maes, The fluctuation theorem as a Gibbs property, J. Stat. Phys. **95**, 367 (1999).
[42] J. L. Lebowitz and H. Spohn, A Gallavotti–Cohen-type symmetry in the large deviation functional for stochastic dynamics, J. Stat. Phys. **95**, 333 (1999).
[43] M. Esposito and C. Van den Broeck, Three Detailed Fluctuation Theorems, Phys. Rev. Lett. **104**, 090601 (2010).
[44] S. M. Fielding, M. E. Cates, and P. Sollich, Shear banding, aging and noise dynamics in soft glassy materials, Soft Matter **5**, 2378 (2009).
[45] See Supplemental Material at http://link.aps.org/supplemental/10.1103/PhysRevE.105.L052601 for details on analytical derivations and numerical simulations.
[46] H. J. Barlow, J. O. Cochran, and S. M. Fielding, Ductile and Brittle Yielding in Thermal and Athermal Amorphous Materials, Phys. Rev. Lett. **125**, 168003 (2020).
[47] C. W. Gardiner, *Handbook of Stochastic Methods for Physics, Chemistry and the Natural Sciences*, Springer Series in Synergetics Vol. 13, 3rd ed. (Springer, Berlin, 2004).
[48] D. J. Evans, E. G. D. Cohen, and G. P. Morriss, Probability of Second Law Violations in Shearing Steady States, Phys. Rev. Lett. **71**, 2401 (1993).
[49] G. Gallavotti and E. G. D. Cohen, Dynamical Ensembles in Nonequilibrium Statistical Mechanics, Phys. Rev. Lett. **74**, 2694 (1995).
[50] S. Aumaître, S. Fauve, S. McNamara, and P. Poggi, Power injected in dissipative systems and the fluctuation theorem, Eur. Phys. J. B **19**, 449 (2001).
[51] J. Farago, Injected power fluctuations in Langevin equation, J. Stat. Phys. **107**, 781 (2002).
[52] K. Feitosa and N. Menon, Fluidized Granular Medium as an Instance of the Fluctuation Theorem, Phys. Rev. Lett. **92**, 164301 (2004).
[53] A. Puglisi, P. Visco, A. Barrat, E. Trizac, and F. van Wijland, Fluctuations of Internal Energy Flow in a Vibrated Granular Gas, Phys. Rev. Lett. **95**, 110202 (2005).
[54] L. F. Cugliandolo, The effective temperature, J. Phys. A: Math. Theor. **44**, 483001 (2011).
[55] T. Ekeh *et al.* (unpublished).
[56] M. L. Falk and J. S. Langer, Deformation and failure of amorphous, solidlike materials, Annu. Rev. Condens. Matter Phys. **2**, 353 (2011).
[57] O. Sedes, A. Singh, and J. F. Morris, Fluctuations at the onset of discontinuous shear thickening in a suspension, J. Rheol. **64**, 309 (2020).